Available online at www.sciencedirect.com
SCIENCE DIRECT®

Physica D 208 (2005) 59–72

PHYSICA D

www.elsevier.com/locate/physd

Bifurcation analysis of magnetic reconnection in Hall-MHD-systems

Holger Homann, Rainer Grauer*

Institut für Theoretische Physik I, Ruhr-Universität-Bochum, 44780 Bochum, Germany

Received 24 May 2004; received in revised form 16 March 2005; accepted 3 June 2005
Available online 1 July 2005
Communicated by C.K.R.T. Jones

Abstract

The influence of the Hall-term on the width of the magnetic islands of the tearing-mode is examined. We applied the center manifold (CMF) theory to a magnetohydrodynamic (MHD)-system. The MHD-system was chosen to be incompressible and includes in addition to viscosity the Hall-term in Ohm's law. For certain values of physical parameters the corresponding center manifold is two-dimensional and therefore the original partial differential equations could be reduced to a two-dimensional system of ordinary ones. This amplitude equations exhibit a pitchfork-bifurcation which corresponds to the occurrence of the tearing-mode. Eigenvalue-problems and linear equations due to the center manifold reduction were solved numerically with the Arpack++-library. An important result of this analysis is the growth of the tearing mode island width by increasing the Hall-parameter, a feature which has been observed in recent numerical simulations of collisionless reconnection.

Keywords: Hall-MHD; Tearing instability; Reconnection; Bifurcation theory; Center manifold theory

1. Introduction

The term magnetic reconnection corresponds to the process of topological reordering of magnetic field lines. This process transfers energy stored in the magnetic field to the surrounding plasma. Magnetic reconnection is one of the most relevant processes in astrophysical, space and laboratory plasmas. Reconnection plays a major role in understanding phenomena like solar flares, small scale dynamos and sawtooth disruptions in tokamaks.

In the last 10 years much progress has been made to understand why collisional reconnection is so fast. A major impact milestone was the comparison of kinetic, hybrid and fluid simulations of two-dimensional reconnection in the GEM framework [1]. One results of this project was that the Hall-term in Ohm's law is responsible for speeding

* Corresponding author.
E-mail address: grauer@tp1.ruhr-uni-bochum.de (R. Grauer).

0167-2789/$ – see front matter © 2005 Elsevier B.V. All rights reserved.
doi:10.1016/j.physd.2005.06.003

up the process due to the existence of whistler waves, which are also responsible to form a X-point structure in the reconnection region (see also [2]). The Hall-term alone is not able to change the topology of the magnetic field lines, so non-ideal terms in Ohm's law are needed like electron inertia, electron pressure or resistivity.

The goal of this paper is to investigate the influence of the Hall-term on the island width of a tearing mode. In order to study this effect on the structure of magnetic reconnection analytically, we considered an equilibrium of a set of MHD-equations and reduced it within the center manifold theory to a low-dimensional system of ordinary differential equations. This was done by [3] for an only resistive MHD-system. The resulting system exhibits a pitchfork bifurcation which we studied against the Hall-parameter.

In contrast to [3] we used the Arpack++-library to solve eigenvalue problems and linear systems which occurred within the center manifold reduction. This library is designed to solve large, sparse eigenvalue problems for only a few eigenvalues. By means of Arpack++ we determined the spectrum of the linearized Hall-MHD-system and checked an important condition for the applicability of the center manifold theory to the underlying MHD-system.

2. The center manifold reduction

The center manifold theory deals with the reduction of a dynamical system in the neighbourhood of a non-hyperbolic fixed point.

Consider a system of ordinary differential equations,

$$\dot{\boldsymbol{x}} = \boldsymbol{f}(\boldsymbol{x}), \quad \boldsymbol{x} \in \mathbb{R}^n, \quad \boldsymbol{f} : \mathbb{R}^n \to \mathbb{R}^n, \tag{1}$$

Let $\boldsymbol{x}_0 = \boldsymbol{0}$ be a non-hyperbolic fixed point of $\boldsymbol{f}$ and $\boldsymbol{A}$ the linearisation of $\boldsymbol{f}$. If the spectrum of $\boldsymbol{A}$ only consists of stable (real part < 0) and marginal (real part $= 0$) eigenvalues, the center manifold theory states that there exists a $\boldsymbol{C}^r$ invariant stable manifold W^{s} and a C^{r-1} invariant center manifold W^{c} at $\boldsymbol{x}_0$ which are tangent to the corresponding eigenspaces. Furthermore the center manifold is attractive, that means that trajectories starting in the neighbourhood of $\boldsymbol{x}_0$ will converge to a trajectory lying in W^{c}. This situation is illustrated in Fig. 1. For an overview on center manifold theory see Carr [4], Guckenheimer and Holmes [5], Chow and Hale [6,7]

If one is only interested in the longtime asymptotic behaviour of a solution it is sufficient to study the dynamics restricted to the center manifold.

In order to apply the center manifold reduction to a bifurcation problem of the Hall-MHD equations one has to incorporate parameters and infinite dimensionality. The first point is achieved by extending the configuration space and the differential Eqs. (1) by a parameter space $\mathbb{R}^l$,

$$\begin{aligned} \dot{\boldsymbol{p}} &= \boldsymbol{0}, \\ \dot{\boldsymbol{x}} &= \boldsymbol{f}(\boldsymbol{x}, \boldsymbol{p}). \end{aligned}$$

Obviously the dimension of the center manifold is enlarged by l.

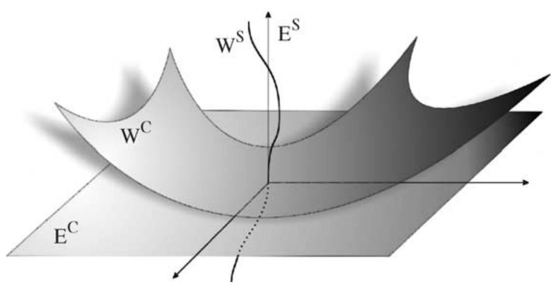

Fig. 1. The invariant manifolds W^{s} and W^{c} at a non-hyperbolic fixed point.

The center manifold theory also applies to infinite-dimensional problems, if certain restrictions are fulfilled, see [8]. For example the spectrum must be decomposed into a part containing a finite number of eigenvalues with real parts equal to zero and a part containing eigenvalues with negative real parts which are bounded away from zero.

For constructing the solution on the center manifold consider a dynamical system given by a PDE

$$\dot{\boldsymbol{u}} = \boldsymbol{f}(\boldsymbol{u}, \boldsymbol{p}), \quad \boldsymbol{f}: \text{ differential operator}, \ \boldsymbol{p} \in \mathbb{R}^l: \text{ parameter space} \tag{2}$$

with the following assumptions. Let $\boldsymbol{u}_0$ be a fixed point of (2) and the spectrum of the linearisation $\boldsymbol{A}$ of $\boldsymbol{f}$ consist of n marginal modes $\boldsymbol{u}^1, \ldots, \boldsymbol{u}^n$, i.e. $\boldsymbol{A}\boldsymbol{u}^i = \omega^i \boldsymbol{u}^i$ with $\mathrm{Re}(\omega^i) = 0$, and eigenvalues with negative real part which are bounded away from zero.

Then an appropriate ansatz for the solution on the center manifold is given by Friedrich [9] and Grauer [3]

$$\boldsymbol{u}(t) = \sum_{i=1}^{n} a_i \boldsymbol{u}^i + \sum_{1 \le j \le k \le n+l} a_j a_k \boldsymbol{u}^{jk} + \sum_{1 \le j \le k \le m \le n+l} a_j a_k a_m \boldsymbol{u}^{jkm} \cdots \tag{3}$$

with

$$\begin{aligned} \dot{a}_1 &= g_1(a_1, \ldots, a_{n+l}) \\ &\ \vdots \\ \dot{a}_n &= g_n(a_1, \ldots, a_{n+l}) \\ \dot{a}_{n+1} &= 0 \\ \dot{a}_{n+l} &= 0 \\ a_{n+i} &= p_i \quad \text{Parameter} \end{aligned} \tag{4}$$

$$g_i = \sum_{j=1}^{n} A_i^j a_j + \sum_{1 \le j \le k \le n+l} A_i^{jk} a_j a_k + \sum_{1 \le j \le k \le l \le n+l} A_i^{jkl} a_j a_k a_l + \cdots \tag{5}$$

The solution (3) is arranged according to the order of the amplitudes a_i. To every order $\mathrm{O}(|a|)$ corresponds a direction of $\boldsymbol{u}^{ij}, \boldsymbol{u}^{ijk}, \ldots$. The amplitudes a_i contain the temporal evolution. However, the expansion (3) only holds for a neighbourhood of $\boldsymbol{u}_0$.

3. The basic equations

In order to investigate the influence of the Hall-term of the Ohm's law on the islands width of the tearing-mode we use a simple MHD-system. It contains in addition to the resistivity the kinematic viscosity which stabilizes the spectrum of eigenvalues of the system. Therefore it is possible to let the spectrum only contain stable and marginal eigenvalues. Furthermore, it is incompressible.

The basic equations are

$$\partial_t \boldsymbol{v} = -(\boldsymbol{v} \cdot \nabla)\boldsymbol{v} + \frac{1}{c\rho_0} \boldsymbol{j} \times \boldsymbol{B} + \nu \Delta \boldsymbol{v} - \frac{1}{\rho_0} \nabla p, \tag{6}$$

$$\partial_t \boldsymbol{B} = -c \nabla \times \boldsymbol{E}, \tag{7}$$

$$\frac{4\pi}{c} \boldsymbol{j} = \nabla \times \boldsymbol{B}, \tag{8}$$

$$\boldsymbol{E} = \frac{m_i}{ce\rho_0} \boldsymbol{j} \times \boldsymbol{B} - \frac{1}{c} \boldsymbol{v} \times \boldsymbol{B} + \eta \boldsymbol{j}, \tag{9}$$

$$\nabla \cdot \boldsymbol{B} = \nabla \cdot \boldsymbol{v} = 0. \tag{10}$$

Using the following notations

$$\boldsymbol{B} \to \bar{B}\boldsymbol{B}, \quad L \to \bar{L}L, \quad \boldsymbol{v} \to v_A \boldsymbol{v}, \quad v_A = \frac{\bar{B}}{\sqrt{4\pi\rho_0}}, \quad t \to \frac{\bar{L}}{v_A}t, \quad \nu \to \rho_0 v_A \bar{L}\nu,$$

$$\eta \to \frac{4\pi v_A \bar{L}}{c^2}\eta, \alpha = \frac{d_i}{L}, \quad \omega_{pi} = \sqrt{\frac{4\pi n_0 e^2}{m_i}}, \quad d_i = \frac{c}{\omega_{pi}}, \quad \rho_0 = m_i n_0,$$

taking the rotation of (6), inserting (8) for $\boldsymbol{j}$ and (9) for $\boldsymbol{E}$ yields

$$\partial_t(\nabla \times \boldsymbol{v}) = \nabla \times (-(\boldsymbol{v} \cdot \nabla)\boldsymbol{v} + (\nabla \times \boldsymbol{B}) \times \boldsymbol{B} + \nu\Delta\boldsymbol{v}) \tag{11}$$

$$\partial_t \boldsymbol{B} = -\nabla \times (\alpha(\nabla \times \boldsymbol{B}) \times \boldsymbol{B} - \boldsymbol{v} \times \boldsymbol{B} + \eta\nabla \times \boldsymbol{B}) \tag{12}$$

$$\nabla \cdot \boldsymbol{B} = \nabla \cdot \boldsymbol{v} = 0 \tag{13}$$

We only consider solutions which are independent of z. Therefore and due to (13) it is convenient to represent $\boldsymbol{v}$ and $\boldsymbol{B}$ by flux functions Φ and Ψ,

$$\begin{aligned} \boldsymbol{v} &= -\nabla \times (\Phi(x, y)\boldsymbol{e}_z) + v_z(x, y)\boldsymbol{e}_z = -\partial_y \Phi \boldsymbol{e}_x + \partial_x \Phi \boldsymbol{e}_y + v_z \boldsymbol{e}_z, \\ \boldsymbol{B} &= -\nabla \times (\Psi(x, y)\boldsymbol{e}_z) + B_z(x, y)\boldsymbol{e}_z = -\partial_y \Psi \boldsymbol{e}_x + \partial_x \Psi \boldsymbol{e}_y + B_z \boldsymbol{e}_z. \end{aligned} \tag{14}$$

An equilibrium of (11) and (12) in terms of the flux functions is given by

$$\Phi_0 = B_{z0} = v_{z0} = 0, \quad \partial_y \Psi_0 = \Psi_0' = F(y), \quad \eta_0 = \frac{E}{\Psi_0''} = \frac{1}{\Psi_0''}, \tag{15}$$

where the prime denotes differentiation with respect to y. Following [3] we set $E = 1$ and choose a Harris-like profile

$$\Psi_0'(y, \lambda) = \tanh(\lambda y) \Rightarrow \Psi_0(y, \lambda) = \frac{1}{\lambda}\ln(\cosh(\lambda y)). \tag{16}$$

We study the problem in a rectangular area $[0, 2\pi] \times [-y_R, y_R]$ with $y_R = 0.5$ and periodic boundary conditions in the x-direction. The geometry and the equilibrium magnetic field are shown in Fig. 2.

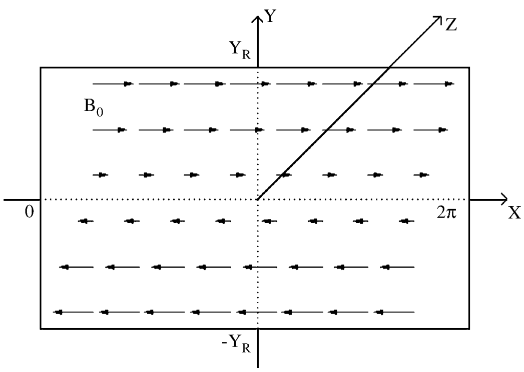

Fig. 2. The geometry of the problem.

After inserting (14) into (11) and (12), the equations for the perturbations of the equilibrium are,

$$\begin{aligned}
\partial_t \Psi &= \eta_0 \Delta\Psi - \Psi_0' \partial_x \Phi - \alpha \Psi_0' \partial_x B_z + [\Psi, \Phi] + \alpha[\Psi, B_z],\\
\partial_t B_z &= -\Psi_0' \partial_x v_z + \eta_0 \Delta B_z + \eta_0' \partial_y B_z + \alpha(\Psi_0' \partial_x \Delta\Psi - \Psi_0''' \partial_x \Psi) + [B_z, \Phi] + [\Psi, v_z] + \alpha[\Delta\Psi, \Psi],\\
\partial_t \Delta\Phi &= \Psi_0''' \partial_x \Psi - \Psi_0' \partial_x \Delta\Psi + \nu \Delta^2 \Phi + [\Delta\Phi, \Phi] + [\Psi, \Delta\Psi],\\
\partial_t v_z &= -\Psi_0' \partial_x B_z + \nu \Delta v_z + [v_z, \Phi] + [\Psi, B_z],
\end{aligned} \tag{17}$$

where we used the standard Bracket

$$[A, B] = \boldsymbol{e}_z \cdot \nabla A \times \nabla B = (\partial_x A)(\partial_y B) - (\partial_y A)(\partial_x B).$$

As in [3] it turns out the boundary condition are not strongly effecting the solutions and for simplicity we impose the following boundary conditions:

$$\begin{aligned}
&\Psi = \Phi = B_z = v_z = 0 \text{ for } y = y_R \text{ and}\\
&\Delta\Phi = \Delta\Psi = 0 \text{ for } y = y_R \text{ and}\\
&\text{all variables } 2\pi\text{-periodic in } x.
\end{aligned} \tag{18}$$

4. Center manifolds of the Hall-MHD-system

In this section the center manifold theory will be applied to the Hall-MHD-system introduced in the previous section. We will study the case that only one eigenvalue becomes marginal. The corresponding eigenspace will be two dimensional due to the translation symmetry in the x-direction.

4.1. The CMF-ansatz

The equations (17) contain the following parameters:

- λ: shear of the equilibrium magnetic field
- ν: viscosity
- α: Hall-parameter

The parameter λ and ν constitute the parameter space. We treat α as an external parameter and use the ansatz (3) with

$$\boldsymbol{u} = \mu = (\Psi, B_z, \Phi, v_z), \tag{19}$$

$$a_3 = \lambda - \lambda^{\mathrm{c}}, \quad a_4 = \nu - \nu^{\mathrm{c}}. \tag{20}$$

4.2. The marginal modes

The linearized problem of (17) is given by

$$\partial_t(\Psi, B_z, \Delta\Phi, v_z) = \mathbf{L}(\Psi, B_z, \Phi, v_z)$$

with the operator

$$\mathbf{L}(\lambda,\nu,\alpha)=\begin{pmatrix} \eta_0\Delta & -\alpha\Psi_0'\partial_x & -\alpha\Psi_0'\partial_x & 0 \\ \alpha[\Psi_0'\partial_x\Delta-\Psi_0'''\partial_x] & \eta_0\Delta+\eta_0'\partial_y & 0 & -\Psi_0'\partial_x \\ \Psi_0'''\partial_x-\Psi_0'\partial_x\Delta & 0 & \nu\Delta^2 & 0 \\ 0 & -\Psi_0'\partial_x & 0 & \nu\Delta \end{pmatrix} \tag{21}$$

and the boundary conditions (18).

Using a Fourier-ansatz like

$$\Psi(x,y)=\sum_k \Psi_k(y)\mathrm{e}^{(\omega_k t+\mathrm{i}kx)}$$

for every variable leads to the following set of ordinary differential equations

$$\begin{aligned} \omega_k\Psi_k &= \eta_0(\Psi_k''-k^2\Psi_k)-\mathrm{i}k\Psi_0'\Phi_k-\mathrm{i}\alpha\Psi_0'kB_{z_k}, \\ \omega_k B_{z_k} &= -\mathrm{i}kv_{z_k}+\eta_0(B_{z_k}''-k^2B_{z_k})+\eta_0'B_{z_k}'+\alpha[\Psi_0'(\mathrm{i}k\Psi_k''-\mathrm{i}k^3\Psi_k)-\mathrm{i}k\Psi_0'''\Psi_k], \\ \omega_k(\Phi_k''-k^2\Phi_k) &= \mathrm{i}k\Psi_0'''\Psi_k-\Psi_0'(\mathrm{i}k\Psi_k''-\mathrm{i}k^3\Psi_k)+\nu(k^4\Phi_k-2k^2\Phi_k''+\Phi_k^{(4)}), \\ \omega_k v_{z_k} &= -\mathrm{i}k\Psi_0'B_{z_k}+\nu(v_{z_k}''-k^2v_{z_k}), \end{aligned} \tag{22}$$

which is a generalized eigenvalue problem for the eigenfunction $\mu_k(y)=(\Psi_k(y), B_{z_k}(y), \Phi_k(y), v_{z_k}(y))$.

We normalize the marginal modes by

$$\langle\langle(\Psi^i,\Phi^i),(\Psi^j,\Phi^j)\rangle\rangle=\delta_{ij}$$

using the scalar product

$$\langle\langle \boldsymbol{A}(x,y),\boldsymbol{B}(x,y)\rangle\rangle=\sum_i\langle A_i(x,y),B_i(x,y)\rangle$$

with

$$\langle A(x,y),B(x,y)\rangle=\int_\Omega A(x,y)\cdot B(x,y)\,\mathrm{d}\tau=\int_{-y_R}^{y_R}\int_0^{2\pi}A(x,y)\cdot B(x,y)\,\mathrm{d}x\,\mathrm{d}y.$$

We examine the case in which only the $k=1$-mode becomes marginal. For every k we computed a few eigenvalues with the largest real part and the corresponding modes. This was done numerically where we dicretised the y-dependence into 256 steps. For solving the dicretised eigenvalue problem we used the Arpack++-Library [10].

Let ω_k^{c} be the eigenvalue with the maximal real part for a given k. An continuous interpolation of the real parts of ω_k^{c} is shown in Fig. 3. We constructed the marginal eigenvalue so that it lies at the local maximum of the interpolated graph. This was done with the simplex-downhill-method and we found the following marginal eigenvalues according to several Hall-parameters.

λ^c	ν^c	α	$\mathrm{Re}(\omega_1^c)$
3.383	5.302×10^{-6}	0	-1.952×10^{-8}
3.369	5.135×10^{-6}	5	1.075×10^{-8}
3.337	4.792×10^{-6}	10	-1.904×10^{-8}
3.300	4.489×10^{-6}	15	-8.516×10^{-9}
3.265	4.315×10^{-6}	20	-2.596×10^{-8}
3.233	4.296×10^{-6}	25	-2.014×10^{-8}

The imaginary part of ω_1^c vanishes for all parameter. The real part of the second greatest eigenvalue is about -0.003, so that a constraint of the applicability of the center manifold theory is fulfilled.

From the complex marginal modes one can construct real modes. Due to the fact that with every solution its complex conjugate is also a solution one obtains the following two real marginal modes:

$$\mu^1 = \begin{pmatrix} \Psi^1 \\ B_z^1 \\ \Phi^1 \\ v_z^1 \end{pmatrix} = \begin{pmatrix} \Psi_1(y)\cos(x) \\ B_{z1}(y)\sin(x) \\ \Phi_1(y)\sin(x) \\ v_{z1}(y)\cos(x) \end{pmatrix}; \quad \mu^2 = \begin{pmatrix} \Psi^2 \\ B_z^2 \\ \Phi^2 \\ v_z^2 \end{pmatrix} = \begin{pmatrix} -\Psi_1(y)\sin(x) \\ B_{z1}(y)\cos(x) \\ \Phi_1(y)\cos(x) \\ -v_{z1}(y)\sin(x) \end{pmatrix} \tag{23}$$

The Figs. 4 and 5 show the computed modes for a couple of Hall-parameters.

One observes that the general structure remains nearly the same, while the amplitudes of the B_{z_1}- and v_{z_1}-modes rise by increasing the Hall-parameter.

4.3. Series expansion of the basic equations

The amplitude equations (3) become easier if one takes into account the symmetries of the problem. The basic equations possess the following symmetries:

- translation T: if $\mu(x, y)$ is a solution of the basic equations, so $T\mu(x, y) = \mu(x + x_0, y)$ as well;
- parity S: if $\mu(x, y)$ is a solution of the basic equations, so $S\mu(x, y) = (\Psi, -B_z, -\Phi, v_z)(-x, y)$ as well.

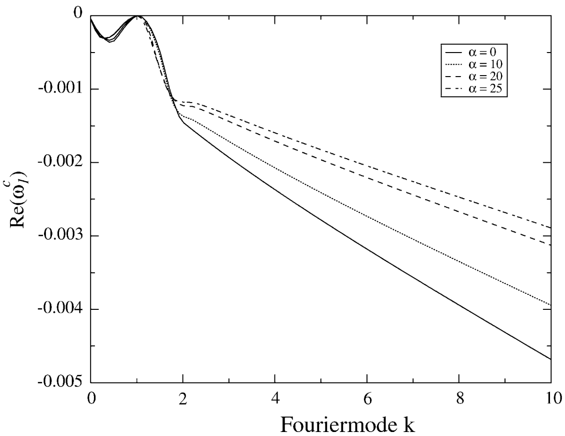

Fig. 3. Real part of ω_k^c vs. k.

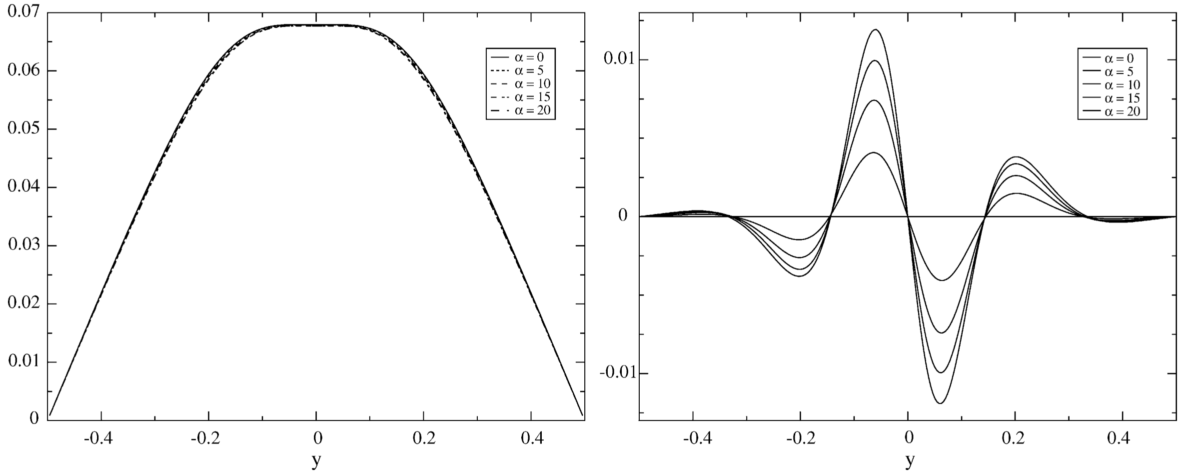

Fig. 4. Marginal Ψ_1 and B_{z_1}-modes for several Hall-parameters, $y_R = 0.5$.

As shown in Sattinger [11] for the Lyaponov–Schmidt procedure and in Grauer [3] for the center manifold theory this symmetries affect the amplitude equations. Due to the symmetries they take the simple form

$$\begin{aligned} \dot{a}_1 &= C_0 a_1 + C_1 a_1 (a_1^2 + a_2^2) \\ \dot{a}_2 &= C_0 a_2 + C_1 a_2 (a_1^2 + a_2^2) \end{aligned} \tag{24}$$

Comparing this with (5) yields

$$\begin{aligned} &C_0 = A_1^{13} a_3 + A_1^{14} a_4 + \cdots, \\ &C_1 = A_1^{111} + A_1^{1113} a_3 + A_1^{1114} a_4 + \cdots, \\ &A_1^{13} = A_2^{23}, \quad A_1^{14} = A_2^{24}, \\ &A_1^{111} = A_1^{122} = A_2^{111} = A_2^{122}, \\ &A_1^{1113} = A_2^{1223} = A_2^{2113}, \end{aligned}$$

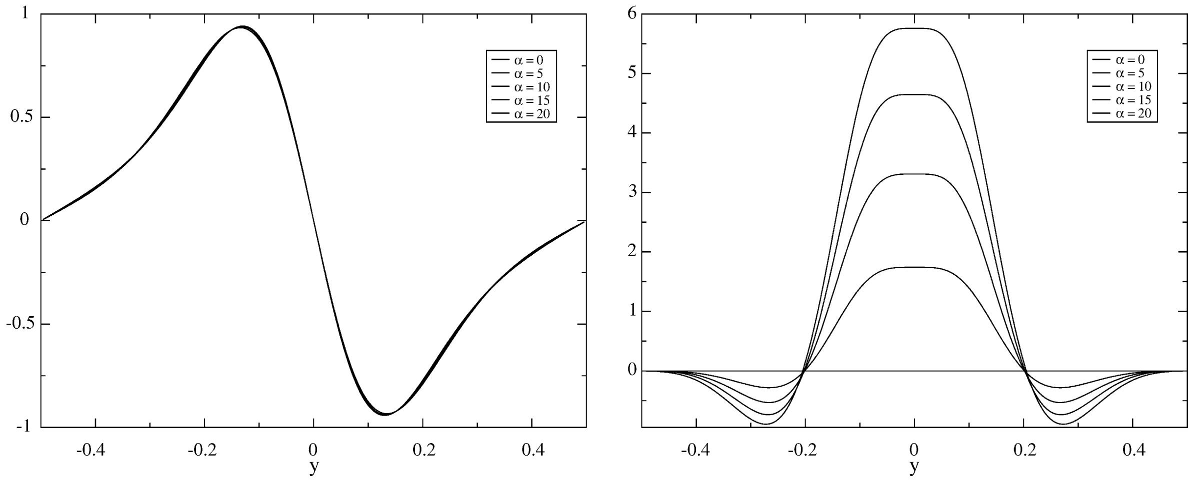

Fig. 5. Marginal Φ_1 and v_{z_1}-modes for several Hall-parameters, $y_R = 0.5$.

Restricting oneself in considering only linear dependence of the coefficients with respect to the parameters (20) one obtains

$$C_0 = A_1^{13}a_3 + A_1^{14}a_4$$
$$C_1 = A_1^{111}$$

In order to study the bifurcation of the equilibrium (15) one only needs to compute the coefficients A_1^{13}, A_1^{14} and A_1^{111}.

Inserting (3) into the basic equations (17) yields equations for every order $\mathrm{O}(|x|)$. Terms of order $\mathrm{O}(|x|^2)$ are:

$$\sum_{1\le i\le j\le 4} a_i a_j \mathbf{L}^{\mathrm{c}} \begin{pmatrix} \Psi^{ij} \\ B_z^{ij} \\ \Phi^{ij} \\ v_z^{ij} \end{pmatrix} = \begin{pmatrix} \Psi^{\mathrm{inh}} \\ B_z^{\mathrm{inh}} \\ \Phi^{\mathrm{inh}} \\ v_z^{\mathrm{inh}} \end{pmatrix} \tag{25}$$

$\mathbf{L}^{\mathrm{c}}$ is the linear operator defined by (21) for the critical parameter values $\lambda = \lambda^{\mathrm{c}}$, $\nu = \nu^{\mathrm{c}}$. The inhomogeneity is given by

$$\begin{aligned}
\Psi^{\mathrm{inh}} &= \sum_{i=1}^{2}\sum_{1\le i\le j\le 4} A_i^{jk} a_j a_k \Psi^i + \sum_{1\le i\le j\le 2}([\Phi^i, \Psi^j] + \alpha[B_z^i, \Psi^j]) - \sum_{i=1}^{2} a_i a_3((\partial_{a_3}\eta_0)|_0(\Delta\Psi^i) \\
&\quad -(\partial_{a_3}\Psi_0)|_0(\partial_x\Phi^i) - \alpha^{\mathrm{c}}(\partial_{a_3}\Psi_0)|_0(\partial_x B_z^i)) \\
B_z^{\mathrm{inh}} &= \sum_{i=1}^{2}\sum_{1\le i\le j\le 4} A_i^{jk} a_j a_k B_z^i + \sum_{1\le i\le j\le 2}([\Phi^i, \Psi^j] + \alpha[B_z^i, \Psi^j]) - \sum_{i=1}^{2} a_i a_3(-(\partial_{a_3}\Psi_0')|_0(\partial_x v_z^i) \\
&\quad +(\partial_{a_3}\eta_0)|_0(\Delta B_z^i) + (\partial_{a_3}\eta_0')|_0(\partial_y B_z^i) + \alpha[(\partial_{a_3}\Psi_0')|_0(\partial_x\Delta\Psi^i) - (\partial_{a_3}\Psi_0''')|_0(\partial_x\Psi^i)]) \\
\Phi^{\mathrm{inh}} &= \sum_{i=1}^{2}\sum_{1\le i\le j\le 4} A_i^{jk} a_j a_k \Phi^i - \sum_{1\le i\le j\le 2}([\Phi^i, \Delta\Phi^j] + [\Delta\Psi^j, \Psi^i]) - \sum_{i=1}^{2} a_i a_3((\partial_{a_3}\Psi_0''')|_0(\partial_x\Psi^i) \\
&\quad -(\partial_{a_3}\Psi_0')|_0(\partial_x\Delta\Psi)) - \textstyle\sum_{i=1}^{2} a_i a_4 \Delta^2\Phi^i \\
v_z^{\mathrm{inh}} &= -\sum_{i=1}^{2}\sum_{1\le i\le j\le 4} A_i^{jk} a_j a_k v_z^i - \sum_{1\le i\le j\le 2}([\Phi^i, v_z^j] + [B_z^j, \Psi^i]) + \sum_{i=1}^{2} a_i a_3(\partial_{a_3}\Psi_0')|_0(\partial_x B_z^i) - \sum_{i=1}^{2} a_i a_4 \Delta v_z^i
\end{aligned}$$

Resolvability of (25) (Fredholm alternative) demands that the inhomogeneity is in the range of L^{c}. This is equivalent to the condition that the inhomogeneity is not in the kernel of the adjoint operator $\tilde{L}^{\mathrm{c}}$. The adjoint operator is given by

$$\tilde{\mathbf{L}}^{\mathrm{c}} = \begin{pmatrix} \eta_0\Delta + 2\eta_0'\partial_y + \eta_0'' & -\alpha\Psi_0'\Delta\partial_x - 2\alpha\Psi_0'''\partial_y\partial_x & \Psi_0'\Delta\partial_x + 2\Psi_0''\partial_y\partial_x & 0 \\ \alpha\Psi_0'\partial_x & \eta_0\Delta + \eta_0'\partial_y & 0 & \Psi_0'\partial_x^2 \\ \Psi_0'\partial_x & 0 & \nu^{\mathrm{c}}\Delta^2 & 0 \\ 0 & \Psi_0'\partial_x & 0 & \nu^{\mathrm{c}}\partial_x\Delta \end{pmatrix} \tag{26}$$

with the boundary conditions

$$\begin{aligned}&\tilde{\Psi}=\tilde{\Phi}=\tilde{B}_z=\tilde{v}_z=0 \text{ at } y=\pm y_R,\\&\Delta\tilde{\Phi}=\Delta\tilde{\Psi}=0 \text{ at } y=\pm y_R \text{ and}\\&\text{all variables are } 2\pi\text{-periodic in } x.\end{aligned}$$

We denote an element of the kernel of $\tilde{L}^{\mathrm{c}}$ by $\tilde{\mu}^{\perp j}=(\tilde{\Psi}^{\perp j}, \tilde{B}_z^{\perp j}, \tilde{\Phi}^{\perp j}, \tilde{v}_z^{\perp j})$ and choose the following normalization

$$\langle\langle(\Psi^i, B_z^i, \Delta\Phi^i, v_z^i), (\tilde{\Psi}^{\perp j}, \tilde{B}_z^{\perp j}, \tilde{\Phi}^{\perp j}, \tilde{v}_z^{\perp j})\rangle\rangle=\delta_{ij}. \tag{27}$$

We computed the kernel of $\tilde{L}^{\mathrm{c}}$ by inserting an Fourier-ansatz. The resulting homogeneous ordinary differential equation has been solved by regarding her as an eigenvalue problem for the eigenvalue zero. Again we treated this problem with the Arpack-library.

Projecting the Eq. (25) onto $\tilde{\mu}^{\perp 1}$ yields the coefficients

$$\begin{aligned}A_1^{13}=&\langle((\partial_{a_3}\eta_0)|_0\Delta\Psi^1-(\partial_{a_3}\Psi_0)|_0\partial_x\Phi^1-\alpha^{\mathrm{c}}(\partial_{a_3}\Psi_0)|_0\partial_x B_z^1), \tilde{\Psi}^{\perp 1}\rangle+\langle(\partial_{a_3}\eta_0)|_0\Delta B_z^1-(\partial_{a_3}\Psi_0')|_0\partial_x v_z^1\\&+(\partial_{a_3}\eta_0')|_0\partial_y B_z^1+\alpha^{\mathrm{c}}((\partial_{a_3}\Psi_0')|_0\partial_x\Delta\Psi^1-(\partial_{a_3}\Psi_0''')|_0\partial_x\Psi^1), \tilde{B}_z^{\perp 1}\rangle+\langle(\partial_{a_3}\Psi_0''')|_0\partial_x\Psi^1\\&-(\partial_{a_3}\Psi_0')|_0\partial_x\Delta\Psi^1, \tilde{\Phi}^{\perp 1}\rangle+\langle(\partial_{a_3}\Psi_0')|_0\partial_x B_z^1, \tilde{v}_z^{\perp 1}\rangle\\A_1^{14}=&\langle\Delta^2\Phi^1, \tilde{\Phi}^{\perp 1}\rangle\end{aligned} \tag{28}$$

In order to compute the coefficient A_1^{111} one has to go to order $\mathrm{O}(|x|^3)$. Once again projecting the resulting equations onto the adjoint kernel yields

$$\begin{aligned}A_1^{111}=&\langle[\Psi^1, \Phi^{11}]+[\Psi^{11}, \Phi^1]+\alpha^{\mathrm{c}}([\Psi^1, B_z^{11}]+[\Psi^{11}, B_z^1]), \tilde{\Psi}^{\perp 1}\rangle+\langle[B_z^1, \Phi^{11}]+[B_z^{11}, \Phi^1]+[\Psi^1, v_z^{11}]\\&+[\Psi^{11}, v_z^1]+\alpha^{\mathrm{c}}([\Delta\Psi^1, \Psi^{11}]+[\Delta\Psi^{11}, \Psi^1]), \tilde{B}_z^{\perp 1}\rangle+\langle[\Psi^1, \Delta\Psi^{11}]+[\Psi^{11}, \Delta\Psi^1]+[\Delta\Phi^1, \Phi^{11}]\\&+[\Delta\Phi^{11}, \Phi^1], \tilde{\Phi}^{\perp 1}\rangle+\langle[v_z^1, \Phi^{11}]+[v_z^{11}, \Phi^1]+[\Psi^1, B_z^{11}]+[\Psi^{11}, B_z^1], \tilde{v}_z^{\perp 1}\rangle.\end{aligned} \tag{29}$$

The unknown “slaved” mode $(\Psi^{11}, B_z^{11}, \Phi^{11}, v_z^{11})$ is given by Eq. (25) with $i=j=k=l=1$. Inserting a Fourier-ansatz yields an ordinary differential equation, which was solved by use of an appropriate function provided by the Arpack-library.

4.4. The amplitude equations

The amplitude equations (24) written in polar coordinates (a, δ), $a, \delta \in \boldsymbol{R}$ are

$$\begin{aligned}&\dot{a}=C_0 a+C_1 a^3,\\&\dot{\delta}=0,\end{aligned} \tag{30}$$

with

$$\begin{aligned}&C_0=A_1^{13}a_3+A_1^{14}a_4,\\&C_1=A_1^{111}.\end{aligned}$$

For $C_1=-1$ this is a normal form of a pitchfork bifurcation at $C_0=0$.

The coefficient C_0 depends on a_3 and a_4. In order to study the general behaviour of the amplitude a of the marginal modes with respect to the Hall-parameter we set $a_4=0$ (keeping the viscosity constant) whereby C_0 only depends on the parameter of the magnetic field λ. Now we choose $\lambda = 0.1$ so that $a_0^2 = -C_0/C_1$ is a fixed point of (30). We computed the equilibrium amplitude a_0 for several Hall-parameters α:

α	a_0 ($\times 10^{-4}$)
0	2.112
5	2.156
10	2.315
15	2.677
20	3.535
25	7.899

The amplitude increases with respect to the Hall-parameter.

Now we can construct the solutions according to this equilibrium amplitudes. Up to first order they are (in polar coordinates)

$$
\begin{aligned}
\Psi &= \Psi_0 + a\Psi_1 \cos(x+\delta),\\
B_z &= aB_{z_1} \sin(x+\delta),\\
\Phi &= a\Phi_1 \sin(x+\delta),\\
v_z &= av_{z_1} \cos(x+\delta),
\end{aligned}
$$

For the visualization we choose $\delta = \pi$. Fig. 6 shows contour plots of the magnetic flux function in $[0, 2\pi] \times [-0.01, 0.01]$ for the Hall-parameter 0 and 25, respectively. The contour lines correspond to the magnetic field lines. Compared to the primary equilibrium (15) they are reconnected. The separatrices separates the magnetic islands from the remaining plasma. They are spread at the magnetic X-point with respect to the Hall-parameter.

The Figs. 7 and 8 show contour plots of B_z, Φ and v_z for $\alpha = 5$ and $\alpha = 25$, respectively (for $\alpha = 0$ the z-components vanish). Here the entire area $[0, 2\pi] \times [-0.5, 0.5]$ is shown. In the case of B_z one observes a quadrupole structure which in numerical [2] simulations is found to be characteristic for the influence of the Hall-term on the reconnection process.

In order to study the influence of the y-dimension on the results we enlarged the y-length of the rectangular area by a factor of 2, this means $y_R = 1$. Now the marginal fix points are about ($\lambda^c = 2.9$, $\nu = 1.5 \times 10^{-3}$).

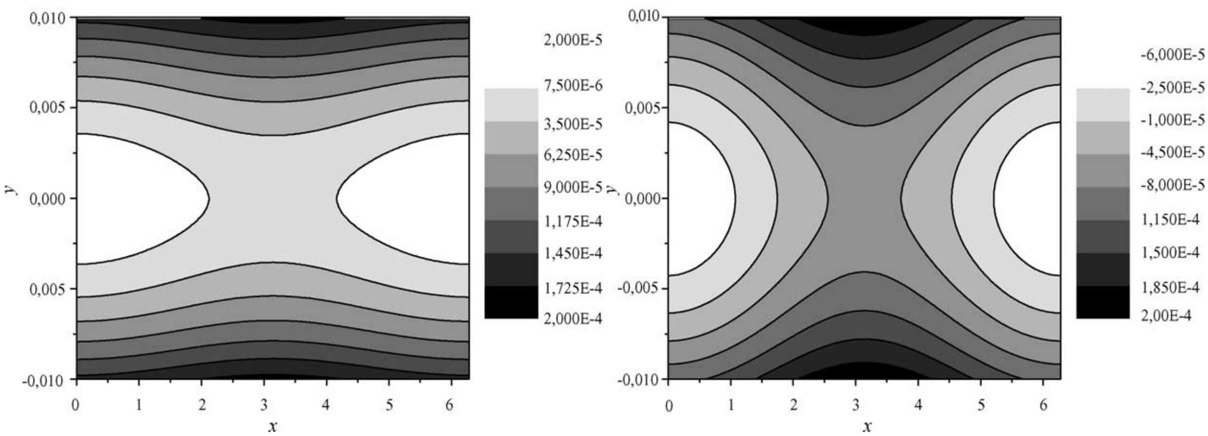

Fig. 6. Contour plot of the magnetic flux function Ψ for $\alpha = 0$ and $\alpha = 25$.

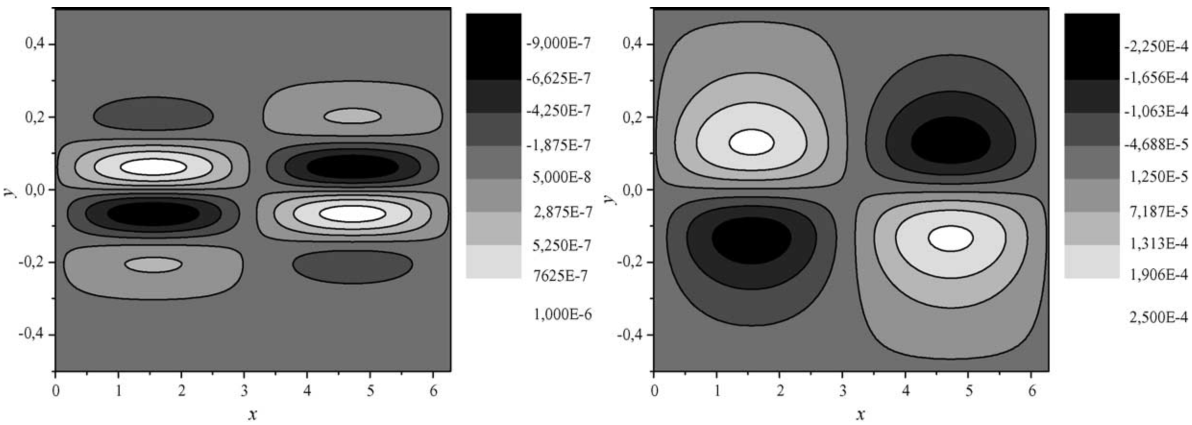

Fig. 7. Contour plot of B_z and for Φ for $\alpha = 5$.

The magnetic field parameter is a little bit smaller and the viscosity about three orders of magnitude greater. Therefore, this configuration is more unstable than the smaller one. The reason for this is the stabilising influence of the boundaries. The boundary condition prescribes that perturbation (the marginal modes) at the boundaries are zero.

For the amplitude a_0 we found in larger case:

α	a_0 $(\times 10^{-3})$
0	8.136
1	8.281
3	9.655
5	17.23

The corresponding marginal modes are given by the Figs. 9 and 10. Here amplitude a_0 is about a factor of 40 greater than in the case of a smaller rectangle with $y_R = 0.5$. The amplitude increases stronger so that even for a Hall-parameter about 3 the effect of the Hall-term is significant.

Furthermore, the shape of the marginal modes changed. They are broadened towards the boundaries.

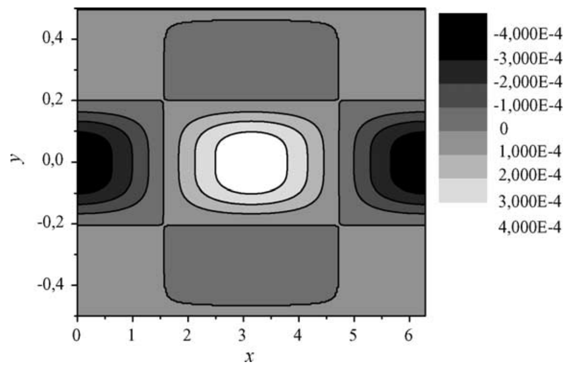

Fig. 8. Contour plot of v_z for $\alpha = 5$.

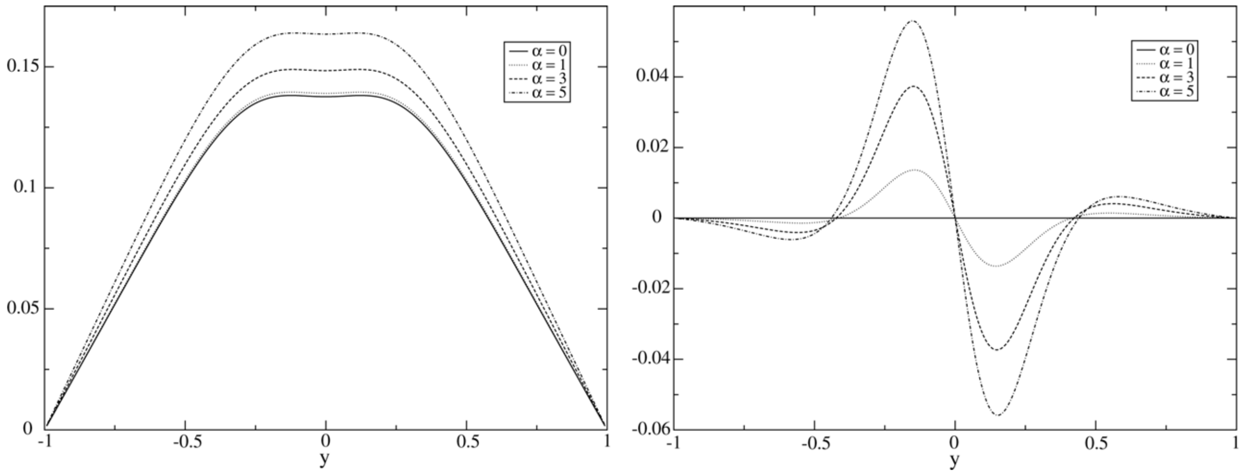

Fig. 9. Marginal Ψ_1 and B_{z_1}-modes for several Hall-parameters, $y_R = 1$.

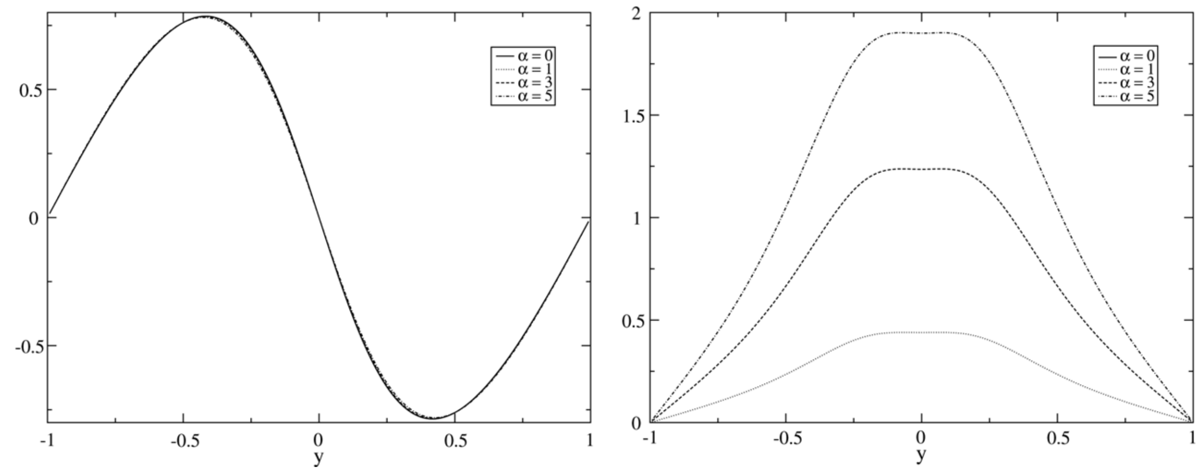

Fig. 10. Marginal Φ_1 and v_{z_1}-modes for several Hall-parameters, $y_R = 1$.

5. Conclusions

In this paper we calculated the influence of the Hall-term on the island width of a tearing instability. This has been done in the framework of a simple model using resistivity as the non ideal process to achieve a change in the topology of the magnetic field. Using center manifold theory, we could calculate the dependence of the tearing mode island width on the Hall-parameter α. The result was an increase of the island width with increasing the strength of the Hall-term. This is in agreement with recent numerical simulations (see [2]), which showed that in contrast to a Sweet-Parker like reconnection in MHD without a Hall-term, the inclusion of a Hall-term could alter the dynamics to a Petschek like behavior with a pronounced X-point in the reconnection zone. In addition, the center manifold reduction could also reproduce the quadrupole like structure of the perpendicular magnetic field (see Fig. 7) as a consequence of the enhanced perpendicular velocity (see Fig. 8) again as observed in numerical simulations. Many nontrivial things still have to come, where the major points are more realistic parameters as in the GEM study and the replacement of resistivity by electron inertia. Work on this is in progress.

Acknowledgements

This work was supported by the SFB 591 of the Deutsche Forschungsgesellschaft and the INTAS program under project number 00292.

References

[1] J. Birn, J.F. Drake, M.A. Shay, B.N. Rogers, R.E. Denton, M. Hesse, M. Kuznetsova, Z.W. Ma, A. Bhattacharjee, A. Otto, P.L. Pritchett, Gem magnetic reconnection challenge, J. Geophys. Res. 106 (2001) 3715.
[2] M. Shay, J. Drake, B. Rogers, R. Denton, Alfvénic collisionless magnetic reconnection and the hall term, J. Geophys. Res. 106 (2001) 3759–3772.
[3] R. Grauer, Nonlinear interactions of tearing modes in the vicinity of a bifurcation point of codimension two, Physica D 35 (1989) 107–126.
[4] J. Carr, Applications of Center Manifold Theory, Springer-Verlag, New York, 1981.
[5] J. Guckenheimer, P. Holmes, Nonlinear Oscillations, Dynamical Systems, and Bifurcations of Vector Fields, Springer-Verlag, Berlin, 1990.
[6] S. Chow, J. Hale, Methods of Bifurcation Theory, Springer-Verlag, Berlin, 1982.
[7] D. Henry, Geometric Theory of Semilinear Parabolic Equations, Lecture Notes in Mathematics, vol. 840, Springer-Verlag, Berlin, 1981.
[8] J.E. Marsden, M. McCracken, The Hopf Bifurcation and its Applications, Springer-Verlag, New York, Heidelberg, Berlin, 1976.
[9] R. Friedrich, H. Haken, Stationary, wavelike, and chaotic thermal convection in spherical geometries, Phys. Rev. A 34 (1986) 2100–2120.
[10] http://www.caam.rice.edu/software/arpack, http://www.ime.unicamp.br/chico/arpack++.
[11] D.H. Sattinger, Group Theoretic Methods in Bifurcation Theory, Springer, Berlin, 1979.